PHYSICAL REVIEW B VOLUME 51, NUMBER 16 15 APRIL 1995-II

Phase coherence and trajectory trapping around one or two independently controllable antidots in quantum wires

C. Gould,* A. S. Sachrajda, Y. Feng, A. Delage, P. J. Kelly, K. Leung, and P. T. Coleridge
Institute for Microstructural Sciences, National Research Council, Ottawa, Canada K1A 0R6
(Received 2 February 1995)

Magnetoconductance measurements have been made on an interesting versatile system. Six independent gates, on a two-dimensional electron-gas heterostructure, are used to define electrostatically two independently controllable antidots within a quantum wire. Measurements in a magnetic field show trapping of trajectories around either a single or a pair of antidots. Collimation, adiabatic transport, and trapping effects combine to create a rich variety of magnetoconductance features which are modulated by large single-period Aharonov-Bohm oscillations at temperatures below 1 K. Experimental features are compared to results from semiclassical ballistic-trajectory models and the similarities and differences between this system and antidot lattices discussed.

The applicability of classical transport theory to smaller and smaller semiconductor devices is of great current interest, e.g., in understanding recent experiments on quantum chaos[1] and finite-size antidot superlattices.[2] In these latter experiments magnetoresistance peaks occur at magnetic fields where the cyclotron orbit and the antidot lattice are commensurate. These peaks were first interpreted by a simple billiard model[2] in which electrons pinned around the antidots were unaffected by weak electric fields and therefore removed from the transport process. A more detailed analysis[3] using a more realistic antidot lattice potential landscape revealed that the peaks could be more closely related to electrons trapped on classically chaotic orbits at the same commensurate magnetic-field values. At very low temperatures Aharonov-Bohm (AB) oscillations were observed by Weiss *et al.*[4] and were explained in terms of several quantized periodic orbits in the antidot lattice potential landscape. Studying smaller antidot lattices in which the phase coherence length was longer than the lattice size, Schuster *et al.*[5] observed AB oscillations related to orbits encircling more than one antidot. In this paper we demonstrate and study pinning in its most basic form. Using a multilevel fabrication technique[6] to electrically contact two individually controllable isolated 0.2-μm-diam gates, we can by appropriate gate activation place one or two antidots inside a quantum wire. The geometry can be configured to produce up to three parallel quantum-point contacts (QPC's). At zero magnetic field we show that the conductance of the QPC's add classically; in low magnetic fields trapping of the cyclotron orbits around the antidots is investigated in some detail and at higher magnetic fields transition to the magnetic edge-state regime is observed.

The device is illustrated schematically in the insets of Fig. 2. Four electrostatic gates are used to define a wide and long quantum wire (lithographically 5 μm long by 1 μm wide) in the two-dimensional electron gas (2DEG) of a GaAs/$Al_xGa_{1-x}As$ heterostructure. The density and mobility of the 2DEG measured in the bulk were 3.2×10^{11} cm^{-2} and approximately 10^6 cm^2/V s, respectively. The two 0.2-μm-diam antidot gates were placed 0.2 μm apart and 0.2 μm from the wires. The measurements were made in a dilution refrigerator using standard low excitation ac techniques.

By using all four wire gates a long quantum wire is formed and using only two diagonal gates a very short wire or constriction (SC) is formed. In each case one or two antidots can be formed within the confining quantum wire.

Two antidots in a wire form three parallel QPC's. Figure 1 shows the effect of forming these in the SC. If the three QPC's are labeled A, B (the middle), and C then curve 1 (G_B) shows the effect of sweeping the two antidot gates when both A and C are pinched off by reducing the width of the quantum wire; curves 2 and 3 (G_{B+C},G_{A+B}) show the effects of pinching off either A or C, and curve 4 (G_{A+B+C}) shows the effect of opening all three. A relatively small background resistance has been subtracted from each measurement. Curve 5, which is the sum ($G_{A+B}+G_{B+C}-G_B$), agrees well with curve 4, i.e., the conductances add classically. A similar result is true for the long wire (curves 6 and 7 in the inset). The results are consistent with previous measurements on two parallel QPC's (Ref. 7) and provide justification for analysis of the magnetoconductance results in terms of the sum of the transmission coefficients of the individual QPC's.

In low magnetic fields, there is the possibility of trapping electrons when there are two or more parallel QPC's. With a single antidot and two QPC's the beams of electrons passing through each are strongly collimated.[8] For particular magnetic-field values part of the collimated beam emerging from one QPC is magnetically focused back through the second (see insets to Fig. 2 for examples). Some of the electron trajectories emerging from the second QPC are then refocused into the original QPC leading to a pinning of the trajectories on the antidot. This reduces the transmission coefficient of the QPC.

This situation is explored in the low-field magnetic resistance data shown in Fig. 2. All data were taken at 100 mK and the insets show schematically the gate configurations. In all cases the conductance of each individual QPC has been set either to zero or $2e^2/h$ throughout the magnetic-field range shown. In Fig. 2(a) where, because of the fringing

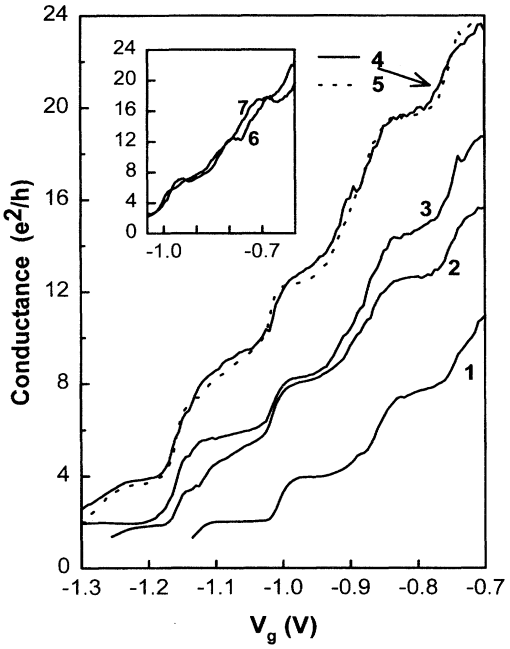

FIG. 1. Antidot gate voltage sweeps in the short constriction (SC) configuration at 1 K. G_B, curve 1; G_{A+B}, curve 2; G_{B+C}, curve 3; G_{A+B+C}, curve 4; $G_{A+B}+G_{B+C}-G_B$, curve 5. The inset shows antidot gate voltage sweeps for the long wire configuration. $G_{A+B}+G_{B+C}-G_B$, curve 6; G_{A+B+C}, curve 7 (see text for details).

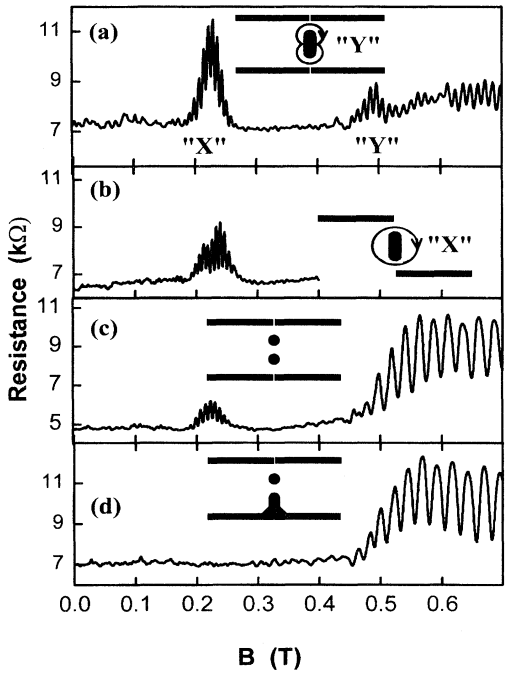

FIG. 2. Magnetoresistance sweeps for different gate configurations (shown in the insets) at 100 mK (each open QPC has a conductance of $2e^2/h$). X and Y refer to trapping peaks. An example of a trajectory for each peak is illustrated in the insets.

electric field of the two antidot gates, the center QPC has been pinched off, two peaks can be seen with, in each case, superimposed oscillations periodic in B. These are not Shubnikov–de Haas oscillations. For the lower (X) peak the period is 7 mT, for the higher peak it is 9 mT but the oscillations persist up to 3 T with a smooth increase in period up to about 11 mT. Below 0.2 T there is a background of reproducible conductance fluctuations. Figure 2(b) shows the corresponding data for the SC, i.e., only with the two diagonal gates activated. In this case the data are very similar except the conductance fluctuations appear to have been suppressed.

In trace 2(c) the center QPC has been opened: the X peak is still present with the 7-mT period oscillations but the Y peak has disappeared and the high-field oscillation period has increased to 25 mT. In trace 2(d) where one of the QPC's has been pinched off, the X peak has vanished but the high field, 25-mT period, oscillations remain.

The low-field conductance fluctuations present in 2(a) but suppressed in 2(b) are associated with quantum interference in the long 5-μm wire and are absent in the SC geometry. The X and Y peaks are identified with trapping around both of the antidots and some classical trajectories involved are sketched in the insets of Figs. 2(a) and 2(b). The trajectories enclose areas significantly larger than the antidot itself and are the first two peaks of a whole series involving an increasing number of reflections off the antidot. Under suitable gate conditions three such peaks could be observed. The number is limited because of the eventual edge-state formation within the QPC's at high magnetic fields. The magnetic fields at which pinning takes place are closely related to the sequence of commensurate magnetic fields observed in antidot lattices. In this present case different peaks involve a different number of collisions around an antidot whereas for the antidot lattice the peaks correspond to different numbers of encircled antidots.

For temperatures below 1 K the X peak is always observed to be modulated by a period of about 7 mT in good agreement with the AB period for the area enclosed by the classical trajectory with a diameter determined by the spacing between the QPC's. By contrast the high-field oscillations (>0.5 T) are resonant modulations of the conductance of the device in the magnetic edge state regime. This is analogous to effects first observed in quantum dots[9] and later in antidots.[10] The area connected with these oscillations is that of the antidots. In Fig. 2(a) the single large antidot area results in a period of around 10 mT but in 2(d), where the individual antidots each have a smaller area, there is a correspondingly larger period of ~ 25 mT. The focusing peak X is missing in Fig. 2(d) because one of the edge QPC's has been pinched off. In Fig. 2(c), where the region between the two antidots is open, the X peak is present with the 7-mT AB modulation. The Y peak is absent, however, because due to the opening between the antidots, no intermediate collision is possible. A weak indication of a second X peak, corresponding to trapping around each individual antidot, was occasionally observed. The higher-field oscillations are determined by the area of each individual antidot and therefore have a period of 25 mT.

To gain further insight into the ballistic trapping behavior we investigated the low-field magnetoresistance dependence on the antidot gate voltage (i.e., we varied the properties of

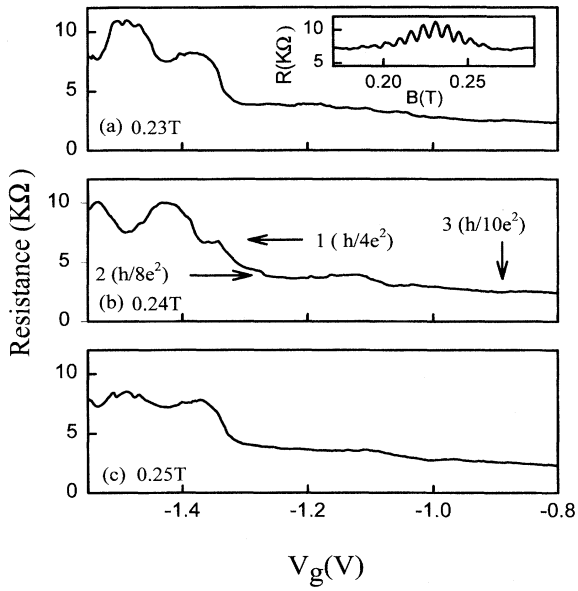

FIG. 3. Resistance measurements as a function of the antidot gate voltage taken at different magnetic fields at 100 mK. For comparison the inset illustrates a field sweep at -1.5 V. The plateaus labeled 1,2,3 in (b) refer to specific QPC configurations (see text for details). The approximate conductance of each plateau is shown in parentheses.

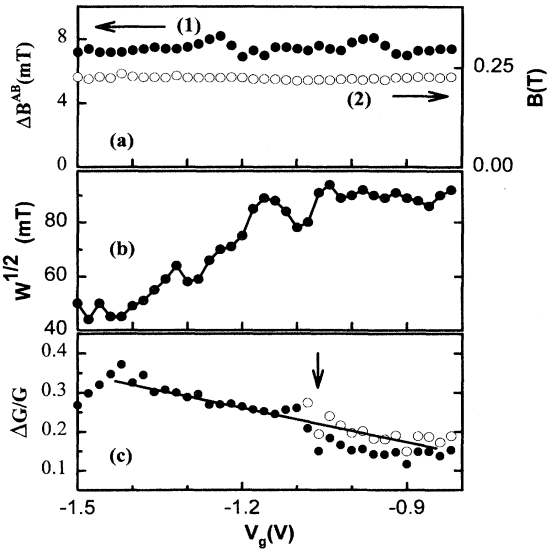

FIG. 4. Results from magnetoresistance sweeps for different antidot gate voltages. (a) The period of the Aharonov-Bohm oscillations superimposed on the X peak (curve 1) and the field position of the X peak (curve 2). (b) The half-width of the X peak. (c) The relative magnitude of the X peak (the ratio of the magnitude of the X peak to the total conductance). The arrow is drawn at the voltage at which the center QPC opens. The open symbols are obtained from the data by adding $2e^2/h$ to the total conductance (see text for details). The line is a guide to the eye.

the QPC's). Because of the many possible configurations the conductances of the outside two QPC's were arranged to be equal to each other (by making a small adjustment to the voltage difference between the two antidot gates) and could then be kept equal by sweeping the two antidot gates together. Figure 3 shows the results of such sweeps at three fields corresponding to different places on the X peak. Three plateaus are observed [see Fig. 3(b)] corresponding to (1) a single (spin unresolved) mode in each outer QPC with the center QPC pinched off (resistance $\sim h/4e^2$), (2) two modes in each of the outer QPC's with the center pinched off (resistance $\sim h/8e^2$), and (3) two modes in the outer QPC's and one in the center (resistance $\sim h/10e^2$). These results are consistent with the results of separately calibrating each QPC.

The properties of the X peak (measured at different gate voltage values) and the period of the associated AB oscillations are shown in Fig. 4. Somewhat surprisingly the period of the AB oscillations and the position of the X peak are essentially independent of gate voltage although the peak narrows and the relative magnitude of the peak (i.e., the ratio of the peak to total conductance) increases as the QPC's are gradually pinched off. The open symbols in Fig. 4(c) are plotted in the regime where the center QPC is open. They are obtained by adding $2e^2/h$ to the total conductance. The resultant smooth trend in the data supports our assumption that the only role the center QPC plays in this field regime is to contribute $2e^2/h$ to the total conductance.

The X peak was investigated by modeling using semiclassical ballistic trajectory analysis[11] with a hard-wall potential. The conductance of each edge QPC was obtained by examining the number of trajectories that were magnetically focused through the other edge QPC. For simplicity all trajectories which successfully passed once through both QPC's were assumed trapped—i.e., no distinction was made between chaotic and nonchaotic trajectories nor between trajectories involving a different number of orbits. Two models were used to characterize the QPC's; in $M1$ a simple cone of acceptance[8] at the narrowest point of the QPC was used (equal to the angular spread of the emitted beam of electrons at the exit of the QPC's); in $M2$ all the various collimating processes were included by defining a cone of acceptance and emittance[8] at the widest part of the QPC's (i.e., the entrances and exits). To fit the field position of the peak the required density away from the QPC's was close to the bulk density for $M1$ but about 30% lower for the $M2$ model. Appealing to the results shown in Figs. 1 and 4(c), the total conductance of the device was taken as the sum of the conductances of each QPC. The relative magnitude and half-width dependencies could be qualitatively explained in both models in terms of an increase in collimation as the QPC's are pinched off, although to explain the saturation behavior for the narrowest QPC's (< -1.4 V) requires the assumption of diffraction limiting the collimation. For the realistic cone of acceptance angles[8] $M1$ reproduced the height but underestimated the width of the X peak, while $M2$ overestimated the width and height by up to 40%. Several features of the data, in particular, the gate voltage independence of the peak position, could only be duplicated by the model $M2$. Generally, the simple semiclassical trajectory model gave a surprisingly good qualitative description of the experimental data; more details will be given elsewhere.

Comparing the classical trajectories predicted by these

hard-wall potential models with the superimposed AB oscillations leads to an unexpected discrepancy. $M1$, for example, predicts that, even with a narrow cone of acceptance ($\pm 17°$), there should be around 100% variation in the areas enclosed by the different trajectories encircling the antidot as a result of the randomizing effects of scattering off the hard-wall potential around the QPC's. From the width of the Fourier transform of the AB oscillations superimposed on the X peaks, however, it is possible to make an estimate for the upper limit in the spread of areas. This turns out to be only 10–15 % for the narrowest QPC's, i.e., an order of magnitude smaller than predicted.

Experimentally, Fig. 4(a), the period of the AB oscillations, and the X peak field position are independent of gate voltage, so the area enclosed by the trajectories is insensitive to changes in the antidot gate voltage (the area would need to change by about 4% to change the enclosed flux quanta by 1). However, oscillations can also be observed as a function of gate voltage when only one mode is occupied in each edge QPC; they appear in Fig. 3 as two peaks on the plateau (1). It is suggested, therefore, that these oscillations are associated not with the magnetic AB phase but rather with phase changes associated with density changes, induced in the QPC's by changes in the gate voltages changing the optical path length of the electron trajectories. This is essentially the same mechanism observed in the interference experiments of Yacoby *et al.*[12]

To summarize, we have fabricated a device involving multiple isolated submicrometer gates and used it to study electron trapping around single and pairs of antidots within a quantum wire. At low magnetic fields magnetoresistance peaks associated with the trapping of classical electron trajectories around one or two antidots are observed and at low temperatures the peaks are modulated by single-period Aharonov-Bohm oscillations. The results were analyzed by a comparison to a ballistic electron trajectory model.

We would like to acknowledge useful discussions with G. Kirczenow, C. R. Leavens, C. Dharma-wardana, and M. Heiblum, and the skillful assistance of P. Marshall in the fabrication of the device and P. Zawadski for help with the cryogenics.

---

*Also at Département de Physique and CRPS, Université de Sherbrooke, Sherbrooke, Québec, Canada J1K 2R1.

[1] C. M. Marcus *et al.*, Phys. Rev. Lett. **69**, 506 (1992).
[2] D. Weiss *et al.*, Phys. Rev. Lett. **66**, 2790 (1991).
[3] R. Fleischmann, T. Geisel, and R. Ketzmerick, Phys. Rev. Lett. **68**, 1367 (1992).
[4] D. Weiss *et al.*, Phys. Rev. Lett. **70**, 4118 (1993).
[5] R. Schuster *et al.*, Phys. Rev. B **49**, 8510 (1994).
[6] Y. Feng *et al.*, Appl. Phys. Lett. **63**, 1666 (1993).
[7] P. J. Simpson *et al.*, Appl. Phys. Lett. **63**, 3191 (1993).
[8] C. W. J. Beenakker and H. van Houten, Phys. Rev. B **39**, 10 445 (1989).
[9] B. J. van Wees *et al.*, Phys. Rev. Lett. **62**, 2523 (1989).
[10] G. Kirczenow *et al.*, Phys. Rev. Lett. **72**, 2069 (1994).
[11] H. U. Baranger *et al.*, Phys. Rev. B **44**, 10 637 (1991).
[12] A. Yacoby *et al.*, Phys. Rev. Lett. **66**, 1938 (1991).